NeuroImage 138 (2016) 221–232

Contents lists available at ScienceDirect

NeuroImage

journal homepage: www.elsevier.com/locate/ynimg

BOLD fMRI in awake prairie voles: A platform for translational social and affective neuroscience

J.R. Yee [a,b,*,1], W.M. Kenkel [a,b,1], P. Kulkarni [a], K. Moore [a], A.M. Perkeybile [a], S. Toddes [a], J.A. Amacker [a], C.S. Carter [b], C.F. Ferris [a]

[a] Dept. of Psychology, Northeastern University, United States
[b] Kinsey Institute, Indiana University, United States

ARTICLE INFO

Article history:
Received 28 April 2016
Revised 14 May 2016
Accepted 17 May 2016
Available online 27 May 2016

Keywords:
Prairie voles
Awake fMRI
Novel odor

ABSTRACT

The advancement of neuroscience depends on continued improvement in methods and models. Here, we present novel techniques for the use of awake functional magnetic resonance imaging (fMRI) in the prairie vole (*Microtus ochrogaster*) — an important step forward in minimally-invasive measurement of neural activity in a non-traditional animal model. Imaging neural responses in prairie voles, a species studied for its propensity to form strong and selective social bonds, is expected to greatly advance our mechanistic understanding of complex social and affective processes. The use of ultra-high-field fMRI allows for recording changes in region-specific activity throughout the entire brain simultaneously and with high temporal and spatial resolutions. By imaging neural responses in awake animals, with minimal invasiveness, we are able to avoid the confound of anesthesia, broaden the scope of possible stimuli, and potentially make use of repeated scans from the same animals. These methods are made possible by the development of an annotated and segmented 3D vole brain atlas and software for image analysis. The use of these methods in the prairie vole provides an opportunity to broaden neuroscientific investigation of behavior via a comparative approach, which highlights the ethological relevance of pro-social behaviors shared between voles and humans, such as communal breeding, selective social bonds, social buffering of stress, and caregiving behaviors. Results using these methods show that fMRI in the prairie vole is capable of yielding robust blood oxygen level dependent (BOLD) signal changes in response to hypercapnic challenge (inhaled 5% CO_2), region-specific physical challenge (unilateral whisker stimulation), and presentation of a set of novel odors. Complementary analyses of repeated restraint sessions in the imaging hardware suggest that voles do not require acclimation to this procedure. Taken together, awake vole fMRI represents a new arena of neurobiological study outside the realm of traditional rodent models.

Introduction

Rationale

Functional imaging of the brain in awake rodents has proven its utility since its inception nearly two decades ago (Lahti et al., 1998), and has elevated our understanding in a variety of scientific disciplines, including absence seizures (Tenney et al., 2004), maternal care (Febo and Ferris, 2007; Ferris et al., 2005), pain (Yee et al., 2015), reward (Kulkarni et al., 2012), neurodegenerative diseases (Ferris et al., 2014), developmental disorders (Kenkel et al., 2016), and drugs of abuse (Febo et al., 2005, 2004; Febo and Ferris, 2007; Madularu et al., 2015). The utility of functional imaging in rodents is largely translational. High-field functional magnetic resonance imaging (fMRI) has been the primary modality for probing the human brain to identify brain regions and networks whose activity is associated with mental processes. Meanwhile, the ability, historically, to probe the brains of non-human animals with more invasive methods has resulted in a wide gap between human and non-human animal neuroscience literatures. Functional imaging of the brain in awake rodents therefore offers the potential to connect these disparate literatures for the purpose of answering some of psychology's most intractable questions surrounding affect regulation and social behavior.

Neuroimaging in awake rodents can identify brain regions, and networks of associated brain regions, involved in the regulation of affect and behavior (Ferris et al., 2011). Decades of neuroscience research have resulted in short lists of brain regions that regulate basic affective and behavioral functions. For example, the medial preoptic area (MPOA) and amygdala are well-known for their roles in sex behavior

Abbreviations: RSA, respiratory sinus arrhythmia.

* Corresponding author at: Department of Psychology, Center for Translational NeuroImaging, Northeastern University, Boston, Massachusetts 02115-5000. Department of Biology, Kinsey Institute, Indiana University, Bloomington, Indiana 47405, United States.
E-mail address: jsn.r.yee@gmail.com (J.R. Yee).

[1] These authors contributed equally to this work.

http://dx.doi.org/10.1016/j.neuroimage.2016.05.046

(Everitt, 1990) and conditioned avoidance (Davis and Whalen, 2001; Phillips and Ledoux, 1992), respectively. However, activation in these areas is not exclusively stimulated by sex and conditioned avoidance. Ultra-high-field fMRI offers the potential to track activation across the entire brain every few seconds. In so doing, awake neuroimaging fills two important functions for the integrative study of animal behavior (Rubenstein et al., 2014): 1) to provide a degree of built-in positive control since the probing of specific constructs should yield differences in regions hypothesized a priori from a history of previous experiments, and 2) providing a novel list of activated regions across the entire brain. By simultaneously testing existing paradigms while implicating new brain regions that function together in a coordinated neural circuit, fMRI in awake rodents offers the potential to "achieve an optimal balance between explicit hypothesis-testing, and the use of new technologies for exploratory work to promote hypothesis generation" (Rubenstein et al., 2014).

Expanding animal models of social and affective functions: the prairie vole model

There is a long, rich history of advancing our understanding of human nature through comparison with other species (Lorenz, 1950; Schmalhausen, 1949; Schneirla, 1949; Tinbergen, 1963). The depth of our new understanding is typically proportional to the extent to which the study species shares the fundamental attributes in question. Studies concerning neuropsychiatric disorders, in particular, or mental function, more broadly, have not adequately considered the value of non-traditional rodent models as compared to commercially bred rodents ("Sixth report on the statistics on the number of animals used for experimental and other scientific purposes in the Member States of the European Union", 2010). This may be reflected in the relative difficulty with which we have come to understand the biological substrates, and thus the proximate causes, of socioaffective disorders such as anxiety and depression. To further our understanding of disordered affect regulation and the way it unfolds within its proximate environment, as well as its wider ecological context, research on affective processes should include animal models whose behavioral reaction norms (Dingemanse et al., 2010; Fuller et al., 2005; Smiseth et al., 2008) more closely resemble those of humans.

Growing research interest in prairie voles represents an attempt to increase the precision of our understanding of human affect and social cognition by selecting a study species that shares the fundamental social attributes of social monogamy and biparental care of offspring (Stoesz et al., 2013; Strickland and Smith, 2015). Prairie voles share with humans the capacity and propensity to form selective social bonds, both with mates (in the context of socially monogamous adult relationships) and with kin (in the context of both alloparenting and biparental care of offspring). Thus, to the extent that affect regulation occurs within a social context in humans, research with prairie voles represents an opportunity to better model the biological substrates of affect regulation. Furthermore, prairie voles exhibit several physiological commonalities with humans that are particularly relevant to affect. Regulation of autonomic nervous function, a critical determinant of affect, displays a human-like bias towards high parasympathetic tone in prairie voles (Grippo et al., 2007). And in prairie voles, circulating plasma concentrations of oxytocin, a peptide hormone critical to the formation and maintenance of selective social preferences, are within the same range as humans, and are 2–4 times higher than in rats (Kramer et al., 2004).

The purpose of this report is to present a series of experiments that demonstrate the current state of the art with regard to imaging neural activation in prairie voles, an animal model that offers the potential to better understand selective sociality and the ways selectivity organizes physiology, affect, and behavior. We first demonstrate, using methods adopted from mouse imaging (Ferris et al., 2014), that acute hypercapnia elicits the expected broad pattern of activation throughout the brain. We next demonstrate the specificity of our imaging methods by successfully eliciting activation in the contralateral primary somatosensory cortex of anesthetized voles undergoing unilateral whisker stimulation. While we were unable to acclimate voles to the stress of the imaging experience, we observed neural activation in response to a set of novel odors in awake voles undergoing their first imaging experience, demonstrating that the stress of the imaging experience is not severe enough to overwhelm the capacity to respond to novel odors.

Methods

Animals

All subject voles were male descendants of wild prairie voles (F4 generation) captured near Champaign, Illinois. Subjects of 60–90 days of age were maintained on a 14/10 h light/dark cycle on at 06:30 AM in a temperature- and humidity-controlled vivarium. Food (Purina rabbit chow) and water were available ad libitum. Prairie vole offspring remained in their natal group with their parents in large polycarbonate cages (24 × 46 × 15 cm) containing cotton nesting material. Offspring were weaned at 20 days of age, prior to the arrival of the next litter to prevent premature exposure to pups, and then were pair-housed with a same-sex sibling in smaller cages (17.5 × 28 × 12 cm) in a single-sex colony room until testing. All procedures were conducted in accordance with the National Institutes of Health Guide for the Care and Use of Laboratory Animals and were approved by the Northeastern University Institutional Animal Care and Use Committee.

Awake imaging technology

Image acquisition

Experiments were conducted in a Bruker Biospec 7.0 T/20-cm USR horizontal magnet (Bruker, Billerica, MA U.S.A) and a 20-G/cm magnetic field gradient insert (ID = 12 cm). Selection of pulse sequences and associated parameters was done with *Paravision v.5.1* software (Bruker, Billerica, MA U.S.A). Voles were scanned at 300 MHz using a quadrature transmit/receive volume coil (ID 38 mm) that provides excellent anatomical resolution and signal-noise-ratio for voxel-based fMRI in rodents 10–50 g in size (Ferris et al., 2014, 2011). At the beginning of each imaging session a high-resolution anatomical set of images covering the entire brain (posterior to anterior) was collected using a rapid acquisition with relaxation enhancement (RARE) pulse sequence (20 slices; slice thickness, 0.70 mm; field of view (FOV) 2.5 cm; data matrix 256 × 256; repetition time (TR) 2.5 s; echo time (TE) 12.0 ms; effective TE 48 ms; number of averages (NEX), 2; total acquisition time, 80 s).

Maintaining neuroanatomical fidelity in the functional scans is important in any imaging study, and is particularly critical here since: 1) we are imaging activity in brains very small in size, and 2) awake voles exhibit a high degree of motion. The neuroanatomical fidelity of our functional scans can be seen when presented alongside the same animal's anatomical scan (see example, Fig. 1). To achieve anatomical fidelity across scans that encompass the whole brain, we chose to use spin echo pulse sequences that were developed for awake imaging in rats and mice (Ferris et al., 2011). In relation to the more common gradient echo BOLD, spin echo BOLD offers several major advantages: i) the potential of improved functional spatial resolution since functional signal changes are localized to the capillary bed, and ii) elimination of magnetic susceptibility artifacts, particularly signal dropout at the interface of air-filled sinus and gray matter (Norris, 2012). Specifically, we used a single-shot fast spin echo/rapid acquisition with relaxation enhancement (FSE/RAREst) pulse sequence with half-Fourier transform that provided reasonable in-plane spatial resolution (260 μm^2), sufficiently thin slices (700 μm/slice), and scans of the entire brain (20 slices) in <6 s. The major disadvantage to spin echo BOLD is low sensitivity, but this is addressed by using a high magnetic field strength (7 T). In addition, and importantly, FSE/RAREst scans run at high magnetic field strengths (7 T and above) result in BOLD signal dominated by the

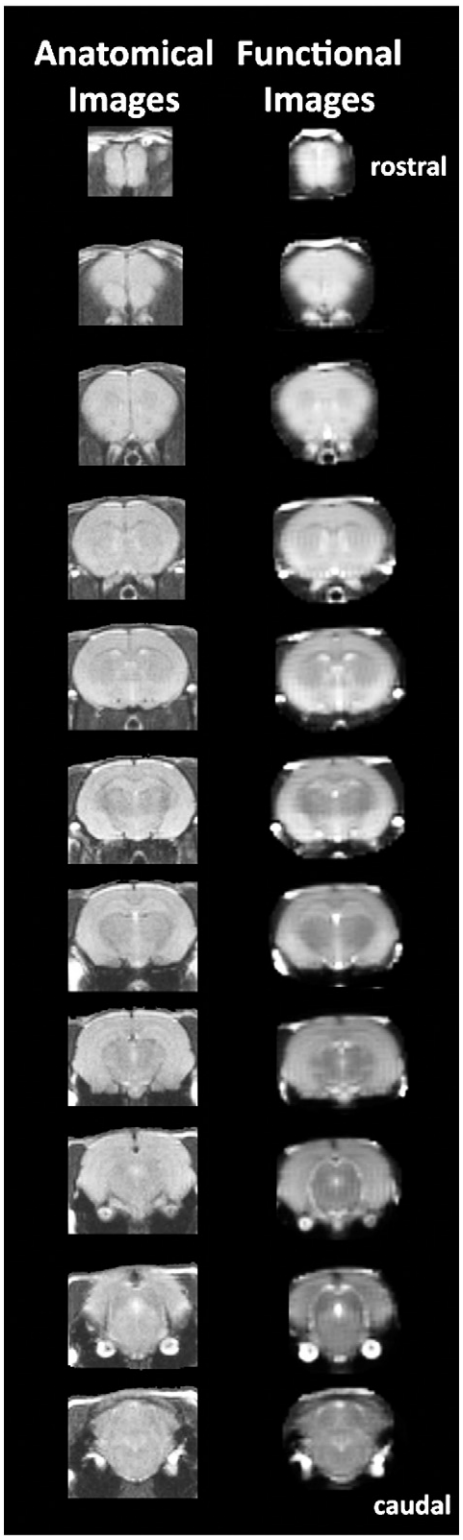

Fig. 1. Anatomical fidelity in functional images. Shown are representative examples of brain images collected during a single imaging session using a multi-slice spin echo, RARE (rapid acquisition with relaxation enhancement) pulse sequence. The column on the left shows axial sections collected during the anatomical scan taken at the beginning of each imaging session using a data matrix of 256 × 256, 20 slices in a field of view of 2.5 cm. The column on the right shows the same images but collected for functional analysis using HASTE, a RARE pulse sequence modified for faster acquisition time. These images were acquired using the same field of view and slice anatomy but a larger data matrix of 96 × 96. Note the anatomical fidelity between the functional images and their original anatomical image. The absence of any distortion is necessary when registering the data to atlas to resolve 115 segmented brain areas.

extravascular dynamic averaging component of the T2-weighted signal (Duong et al., 2003; Ugurbil et al., 2000; Yacoub et al., 2003). The extravascular signal surrounding capillary beds and small vessels is more reflective of the metabolic changes in brain parenchyma than signal from large draining veins and thus provides a more accurate measure of neuronal activity (Yacoub et al., 2007). A second disadvantage of spin echo BOLD is that, even with the advancement of parallel imaging techniques combined with partial Fourier acquisition and the associated shortening of scan times, complete coverage of a large brain, like the human is not possible at sufficiently short repetition times (TR) for event-related fMRI. However, we are able to circumvent this disadvantage given the substantially smaller brain size of rodents and the use of a single epoch stimulus-presentation period.

Multi-slice FSE/RAREst using a partial Fourier acquisition with 9/16 ratio pulse sequences were run with Bruker *Paravision v.5.1*. With this pulse sequence we imaged the entire brain, collecting 20 axial slices per repetition, at 0.70 mm thick, in 6 s repetition intervals (20 slices; slice thickness, 0.70 mm; FOV 2.5 cm; data matrix 96 × 96; repetition time (TR) 6 s; echo time (TE) 2.67 ms; effective TE 40 ms; RARE factor, 62; NEX, 1). With a FOV of 2.5 cm and a data matrix of 96 × 96, the in-plane pixel functional resolution for these studies was 260 μm^2. In automated fashion, *Paravision v.5.1* finds the basic frequency, shims, determines power requirements for 90° and 180° pulses, and sets the receiver gain proportionally. Each single-epoch, event-related scanning session was run in continuous fashion.

Awake imaging hardware

Subjects are restrained for imaging using custom-designed, non-magnetic, non-RF reactive plastic restraint tubes (Animal Imaging Research, Holden, MA, USA), pictured in Fig. 2. The quadrature transmit/receive volume coil (ID 38 mm) provides an excellent anatomical resolution with complete coverage of the brain and olfactory bulbs (Fig. 3). In this arrangement, subjects' heads are immobilized via three elements: an incisor bite bar, which prevents the subject from retreating backwards; a beveled nose cone, which anchors the anterior portion of the head; and a foam helmet, which is squeezed in place upon insertion of the restraint tube into the coil chassis, and thereby anchors the posterior portion of the head. This arrangement minimizes movements of the head and eliminates the ear-bars and pressure points that have been traditionally associated with awake animal imaging. The use of foam helmets with varying shapes/thicknesses allows the experimenter to individually tailor the restraints for each subject, dependent on their size. The nose cone is perforated so as not to restrict the flow of air from the nostrils or mouth. Furthermore, the incisor bite bar also serves as a route of administration for olfactory stimuli or gases as detailed

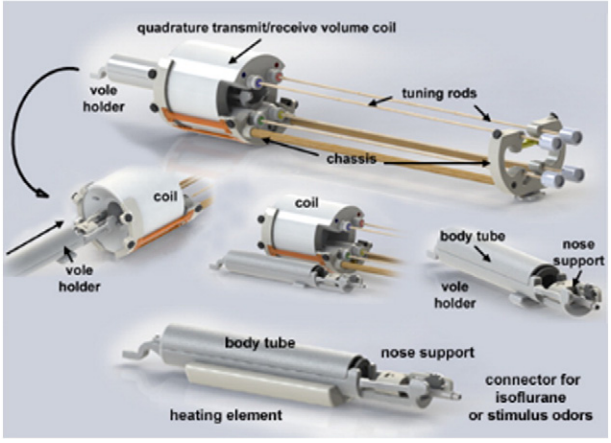

Fig. 2. Vole imaging system. Shown are the different components of the vole imaging system. Note the nose support which includes a hollow tube to secure the front incisors. It is through this tube that odors or volatile anesthetics can be delivered.

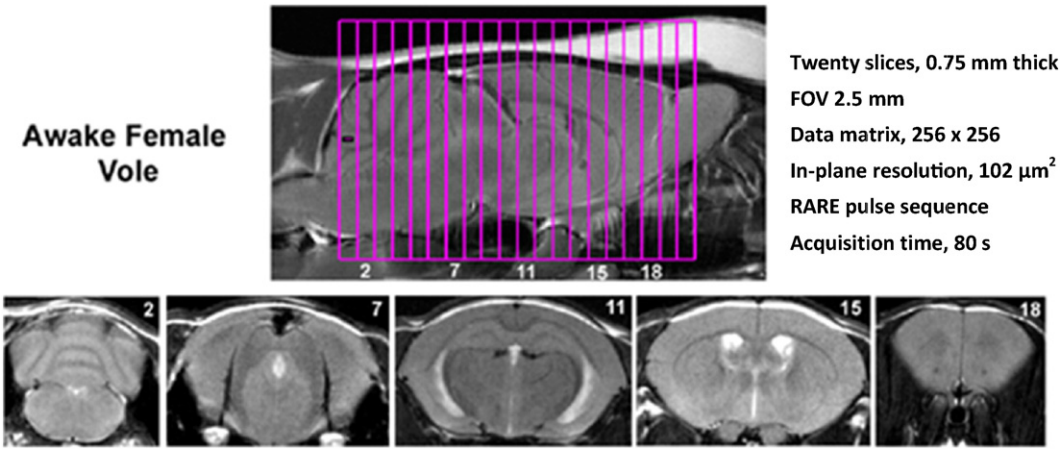

Fig. 3. Field of view and homogeneity. Shown are sagittal and axial views of an awake vole brain. Note the linearity along the Z-axis. The axial images taken from a 20-slice RARE sequence (.75 mm thickness) demonstrate complete brain coverage from the olfactory bulbs to the brainstem. The vole system was provided by *Animal Imaging Research*, Holden, MA, USA.

below. A hollow tube extends from the tip of the nose cone providing a route for administering volatile anesthetics (e.g., isoflurane, carbon dioxide gas) or odors. The entire process of removing a subject from its home cage and preparing it for scanning takes less than a minute. After each imaging session, the equipment is washed and cleaned for the next subject.

Vole brain atlas

A completely new, high-resolution T2-weighted MRI-based brain atlas was developed specifically for the prairie vole, following Paxinos mouse atlas nomenclature (Paxinos and Franklin, 2004). This annotated, 3D segmented atlas consists of 115 brain regions and was created based on the composite of scans from 6 adult voles that underwent high-resolution anatomical scans. Each high-resolution anatomical data set for the atlas was collected using the RARE pulse sequence (57 slices; 0.25 mm; FOV 1.5 cm; data matrix 128 × 128; TR 5.3 s; effective TE, 48 ms; NEX, 15; acquisition time, 140 min).

MRI scans from all subjects were registered to a standard MRI scan with affine transform, including final inspection once all were registered to ensure that boundary surfaces of all the scans matched as perfectly as possible. An average scan from all the subjects was created which was used to create a primary template for each slice. MR scans from each subject were embedded as a background image, and major and minor regions were drawn on individual slices of each subject independently consulting the background MR image, its histology, and two-dimensional atlas textbooks (Paxinos and Franklin, 2004; Swanson, 2004). Further drawings from all the subjects were merged together to create an average representative atlas.

Due to inherent characteristics of their creation by freehand drawing, the averaged atlas now in graphic illustrator format does not comply with strict geometric rules which define the entities represented in the atlases or computer drawings. These drawings were converted to a mathematically robust image format and 3D surface models via an automated 3D segmentation algorithm (Kulkarni et al., 2003). This atlas model now can be rotated and deformed to register any MRI image dataset, at which point every pixel in the set of MRI slices is tagged with the fully segmented tissue classification. An example of this composite approach is illustrated in Fig. 4.

Imaging data analysis

Imaging data analysis included four primary steps: 1) preprocessing, including slice timing correction, co-registration, smoothing, detrending; 2) alignment and registration to vole atlas, followed by segmentation; 3) voxel-wise statistical analysis for each individual to identify voxels that experienced a signal change in relation to baseline; 4) group comparisons on the number of activated voxels per ROI. Each functional scan was preprocessed using SPM8's co-registrational code (quality: 0.97; smoothing: 0.35 mm; separation: 0.5 mm) and smoothed using Gaussian smoothing with a full width at half maximum (FWHM) of 0.6 mm. Preprocessed images were aligned and registered to the 3D vole brain atlas using the interactive graphic user interface *Medical Image Visualization and Analysis Software* (*MIVA*, available for download at: ccni.wpi.edu/miva/html). The registration process involved translation, rotation, and scaling independently and in all three dimensions. Matrices that transformed each subject's anatomy were used to embed each slice within the atlas. All pixel locations of anatomy that were transformed were tagged with major and minor regions in the atlas. This combination created a fully segmented representation of each subject within the atlas.

Using voxel-based analysis, the percent change in BOLD signal for each voxel was averaged for each subject. Statistical *t*-tests were performed on each voxel (ca. 15,000 in number) of each subject within their original coordinate system with a baseline threshold of 2% BOLD change to account for normal fluctuation of BOLD signal in the awake rodent brain (Brevard et al., 2003). As a result of the multiple *t*-test analyses performed, a false-positive detection controlling mechanism was implemented at the level of the ROI to limit false detection of activated voxels within each ROI (Genovese et al., 2002). The *t*-test statistics used a 95% confidence level, two-tailed distributions, and heteroscedastic variance assumptions to identify voxels significantly activated in relation to baseline.

A composite image of the whole brain representing the average of all subjects was constructed for each group for ROI analyses, allowing us to look at each ROI separately to determine the % BOLD change and the number of activated voxels in each ROI. Group comparisons were made by comparing the number of activated voxels per ROI. Since the number of activated voxels per ROI did not fulfill parametric assumptions, we compared groups by using a non-parametric Kruskal–Wallis test statistic followed by a Mann–Whitney *U*-test for post-hoc comparisons.

The timing of change from baseline in % BOLD was assessed by group using sequential paired t-tests with a hypothesized difference of 0. Group differences were assessed by one-way ANOVA at each time point to determine when groups started to diverge from one another following stimulus presentation. Tukey–Kramer post-hoc tests were run in the event of the first significant result to determine the onset of pairwise group differences.

Acclimation

Rationale

Motion artifact presents a substantial hurdle to the use of awake animals in fMRI, as motion creates changes in signal intensity that can be

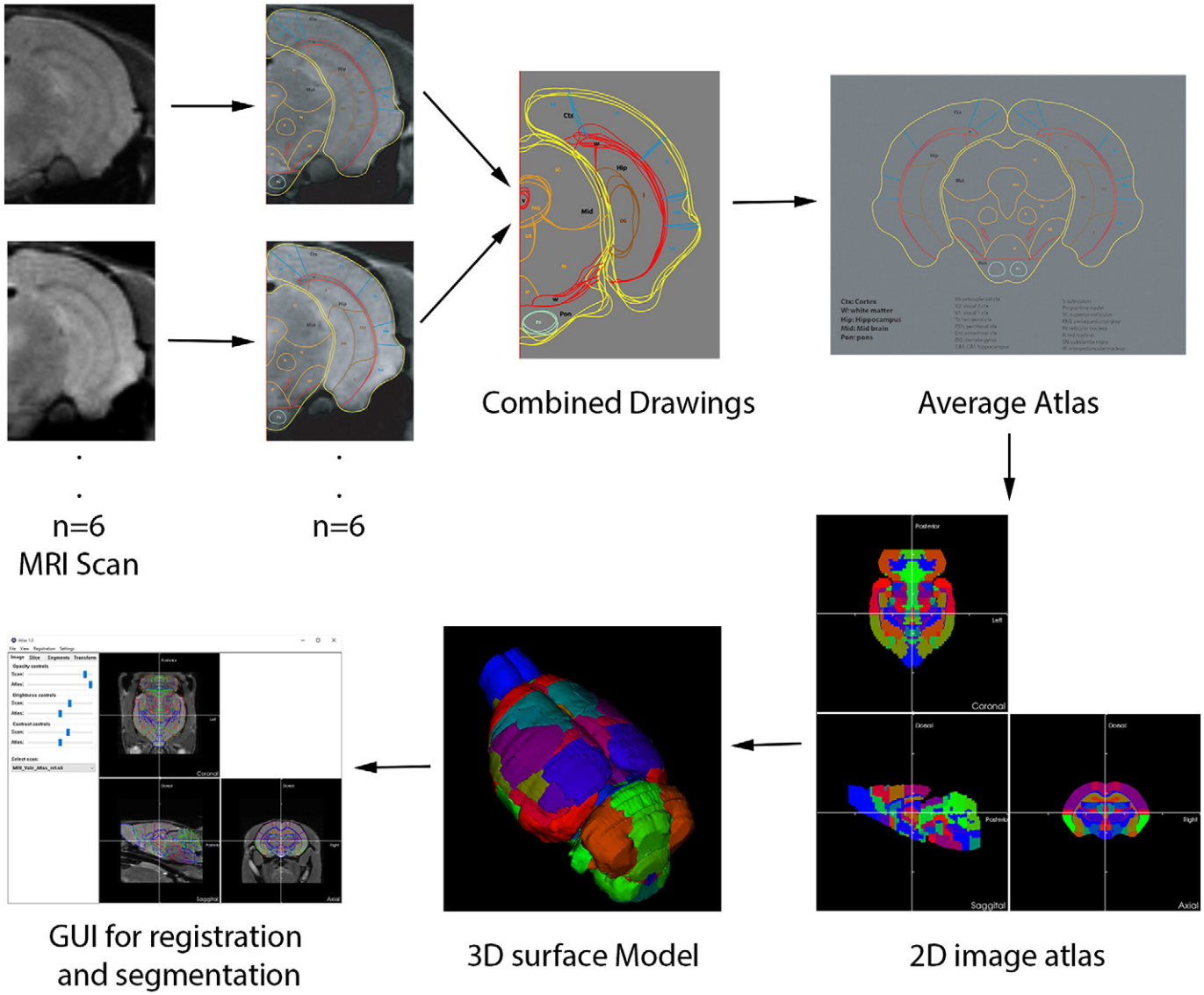

Fig. 4. Vole brain atlas. To create an atlas for the vole brain, high resolution MRI scans from 6 voles were collected and registered to standard MRI with affine transform, inspecting and ensuring that boundary surfaces of all the scans matched as perfectly as possible. Separate brain regions were delineated with freehand drawings for each subject. An average scan from all the subjects was created which was used to create a primary template for each slice. The freehand-drawn average atlas was converted to a mathematically robust image format and 3D surface models via an automated 3D segmentation algorithm. This atlas model now can be rotated and deformed to register any MRI image dataset, at which point every voxel in the set of MRI slices is tagged with the fully segmented tissue classification.

mistakenly attributed to stimulus-induced changes in BOLD signal. Previous work in domesticated rats has shown that repeated daily sessions in a mock-MRI chamber will acclimate the animal to the conditions of restraint (King et al., 2005). This has been demonstrated in rats through gradual reductions in motion artifact, respiratory rate, heart rate, and corticosterone levels. Although acclimation does not eliminate the stress of restraint, it can alleviate some of this confound and reduce the motion artifact present in distressed animals. We therefore sought to examine the effects of a similar acclimation regime in the prairie vole. Acclimation to the conditions of restraint necessary for successful imaging was explored in prairie voles using three distinct approaches: head movement during scanning, measurement of vocalizations and restraint-induced sounds, and recording heart rate/respiratory sinus arrhythmia (RSA). Throughout these studies, acclimation consisted of sessions of 15 min of restraint per day across 5 consecutive days.

Motion data

To most directly test the effects of our acclimation regimen on image stability during image acquisition, prairie voles were scanned on their first and fifth restraint sessions. Adult male prairie voles ($n = 9$) were scanned on days 1 and 5, and acclimated in a mock scanning setup days 2–4 to provide the equivalent of 5 total restraint experiences. Each scan consisted of a 12 min fMRI imaging session preceded by approximately 3 min of setup, including positioning and pilot scans. Acclimation during days 2–4 lasted 15 min and was performed similar to actual fMRI testing, only the restraint apparatus was inserted into a mock scanning tube rather than the actual magnet.

Motion was calculated using the Statistical Parametric Mapping (SPM) MATLAB package, estimated by a 3D rigid body model with 6 degrees of freedom (movement in 3 dimensions and rotation in 3 planes). Data was considered unusable if motion resulted in a disturbance larger than 0.3 mm (a single voxel is 0.260 mm) for more than a single image

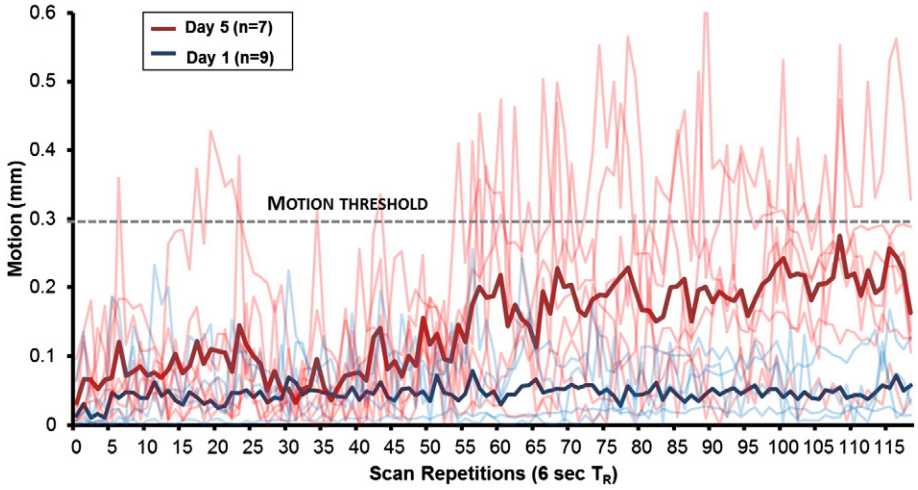

Fig. 5. Motion. Motion during awake animal imaging. Motion for each subject is plotted for subjects naïve to imaging conditions ("Day 1", blue lines, n = 9) as well as following 5 days of repeated restraint ("Day 5", red lines, n = 7); group averages are plotted in bold lines. The acceptable motion threshold of 0.3 mm (dashed line) is slightly smaller than the size of a single voxel. 9 of 9 subjects in the Day 1 condition produced acceptable data, as they did not exceed the motion threshold; 0 of 7 of the Day 5 subjects met this criterion.

acquisition. In order to compare motion between acclimated and non-acclimated subjects, volume-to-volume displacement was averaged within each subject, and subjects were averaged across the absolute value of each dimension of movement (Fig. 5).

Heart rate/RSA

In order to assess the autonomic state of voles during imaging restraint conditions, as well as at rest, a total of eight adult prairie voles (5 males, 3 females) were implanted with radiotelemetry devices according to previously published methods (Kenkel et al., 2013). Briefly, prairie voles were surgically implanted with subcutaneous radiotransmitting devices (ETA-F10, Data Sciences International, St. Paul, MN), which permit the wireless recording of core body temperature, locomotor activity, and electrocardiogram.

Radiotelemetric electrocardiogram data were quantified according to procedures previously described (Grippo et al., 2007; Lewis et al., 2012). Electrocardiogram was sampled at 5000 Hz and visualized in real-time using vendor software (Data Sciences International, St. Paul, MN). Detection and correction of R-waves was verified with CardioEdit 1.5, a custom-designed software package (Brain Body Center, University of Illinois at Chicago). RSA, an index of myelinated vagal input to the heart, was extracted from the time series of R-R intervals using Cardiobatch (Brain–Body Center, University of Illinois at Chicago), a custom-designed software package. RSA was extracted using time domain procedures described in detail elsewhere (Bohrer and Porges, 1982; Grippo et al., 2007; Kenkel et al., 2013; Lewis et al., 2012; Porges, 1985).

Following surgery, subjects recovered across a cage divider from their sibling cage mate for 7 days, followed by an additional 3–7 days without the divider. As part of the acclimation procedure, subjects were tested on 5 consecutive days, which involved recording of baseline, restraint and recovery time periods. Baseline measurements were taken from the 5 min segment most proximal in time to the onset of restraint, and during which time the subject failed to register locomotor activity, as per previously published methods (Kenkel et al., 2013). Restraint lasted 15 min and was performed similar to actual fMRI testing, only the restraint apparatus was inserted into a mock scanning tube of the same diameter rather than the actual magnet. During the 15 min of restraint, the subjects and equipment were placed atop the telemetry receiver boards for data collection. Following return to the home cage, recording was continued for an hour. Here we report heart rate and RSA for both the 5 min of baseline along with the 15 min of restraint. Following return to the home cage, heart rate was averaged across 30 min segments (Fig. 6).

In order to assess the degree of challenge and arousal faced by prairie voles undergoing restraint for imaging, we compared the cardioacceleratory response to commonly used experimental paradigms. Here, we report on heart rate changes induced by 15 min exposures to: the odor of an unrelated pup (1–3 days old) in the home cage; a freely behaving unrelated pup (1–3 days old) in the home cage; and lastly, exposure to a wire mesh floored cage used for urine collection in metabolic studies (Fig. 6c). Data from the pup and pup odor conditions are reprinted with permission from previous work in our lab (Kenkel et al., 2015). All conditions were comprised of 5 adult male and 3 adult females, similar to restraint acclimation.

Vocalizations and escape-related sound

In order to assess the efficacy of our acclimation approach in terms of arousal and distress, adult male and female voles (n = 12 males, 6 females) were recorded throughout the 15 min of restraint that occurred daily for 5 consecutive days. Restraint was performed similar to actual fMRI testing, only the restraint apparatus was inserted into a mock scanning tube rather than the actual magnet. Recordings were made using an Avisoft UltraSoundGate 116Hme microphone, sampling at 96 KHz, 30 cm away from the restrained subject. This arrangement captured both audible and ultrasonic vocalizations emitted, along with sounds produced during escape attempts. Such sounds were detected and quantified using Avisoft-SASlab Pro, version 5.2.07. The total duration as well as number of discrete sounds (typically a combination of vocalization and escape behavior) were summed over each day's 15 min restraint session and then compared across days (Fig. 6c).

Validation stimuli

Hypercapnic challenge

BOLD response to hypercapnic conditions represents a useful positive control to assess a new fMRI protocol as it produces a global increase in BOLD signal throughout the brain (Brevard et al., 2003; Sicard et al., 2003). We have previously used this approach to validate fMRI methods in the rat (Ferris et al., 2008) and mouse (Ferris et al., 2014). In the present study, awake, non-acclimated adult male voles (n = 6) were manually placed in the restraint tube as described above. Scans consisted of three epochs: a 4 min "baseline" epoch, a 4 min "stimulus presentation" epoch, and a 4 min "washout" epoch, for a total of 12 min (120 whole-brain acquisitions). To create

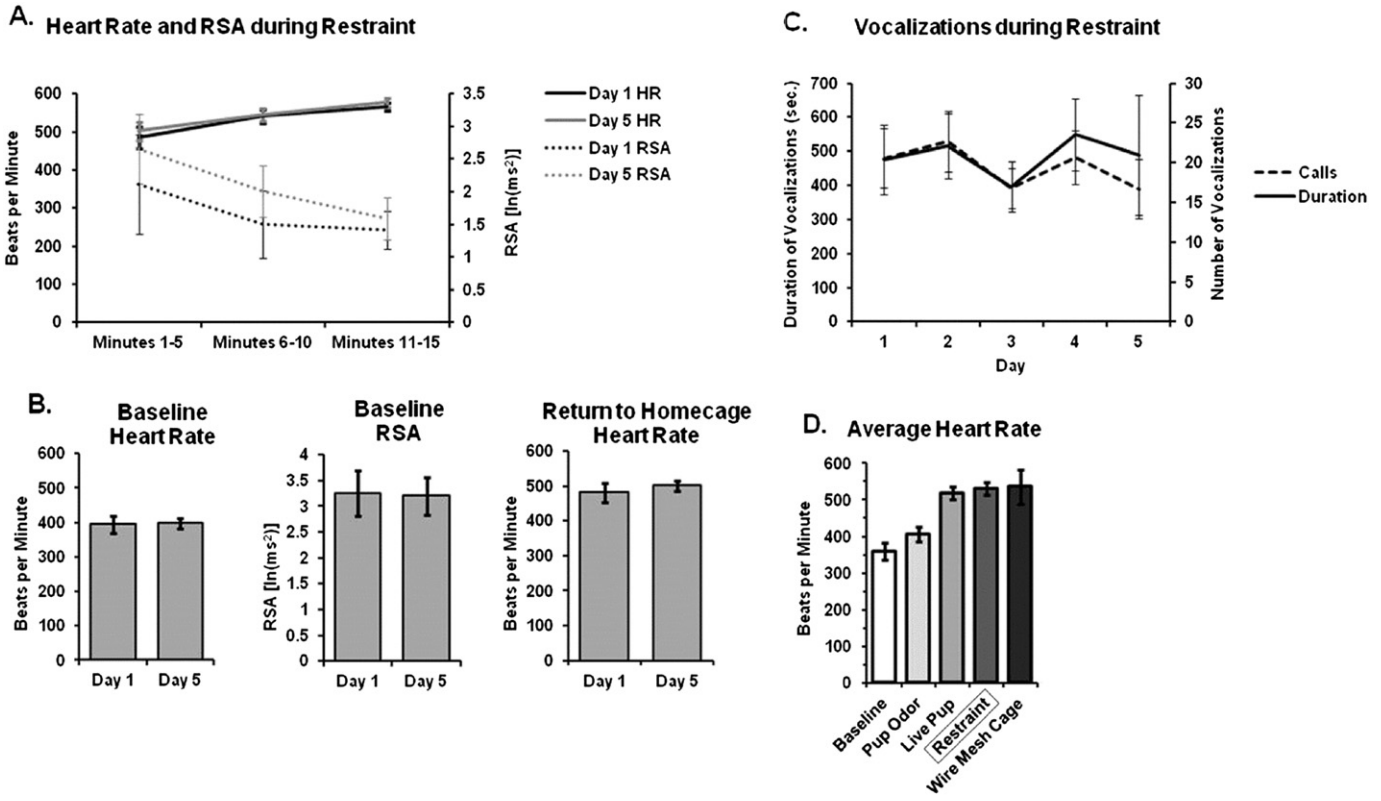

Fig. 6. Acclimation to repeated restraint. (A) Heart rate gradually increased while RSA decreased over the course of a 5 min restraint session; however, there were no differences between days 1 and 5 in either measure. (B) There were no differences in either cardiovascular parameter at baseline, nor following return to the home cage immediately after restraint. (C) Sounds produced during restraint were no different over 5 days of repeated restraint. (D) Average heart rate is shown during restraint in comparison to baseline and various experimental manipulations; heart rate during restraint is roughly similar to that following freely moving exposure to a novel pup or wire mesh floored cage (used for metabolic studies).

hypercapnic conditions, stimulus presentation consisted of a 4 min presentation of 5% CO_2. During baseline and washout, subjects were presented with ambient air at an equivalent flow rate to the CO_2 (~1.5 lpm) (Fig. 7).

Whisker stimulation

As opposed to hypercapnia, which is meant to induce global BOLD signal increase, unilateral stimulation of the whiskers allowed us to test the sensitivity of our imaging methods to detect activation of discrete and specific neural circuits. In this experiment, a separate cohort of non-acclimated adult male prairie voles (n = 8) were anesthetized and scanned in response to either stimulation from a mild air flow across the whiskers on the right side of the face ('Whisker') or no stimulus ('Control'). Subjects underwent both conditions in pseudo-random order. Voles were anesthetized during imaging in this study so that air flow could be applied to the whiskers, which are typically occluded by the restraint hardware. In addition, anesthetizing the voles functioned to minimize the neural response to whisker stimulation, allowing demonstration of the sensitivity of our methods to mild stimuli. Anesthesia was maintained via 1–1.5% isoflurane and monitored via respirometer (SA Instruments, Inc.; Stony Brook, NY, USA). Air flow was applied in a continuous stream and positioned directly at the tips of the vibrissae on the right side of the proboscis (all vibrissae were left intact). Ambient room air from outside the magnet room was pumped directly into the bore of the magnet using polyethylene tubing connected to an aquarium pump. This generated a continuous stream of air flowing at approximately 2 lpm. As above, scans consisted of three epochs: a 4 min "baseline" epoch, a 4 min "stimulus presentation" epoch, and a 4 min "washout" epoch, for a total of 12 min (120 whole-brain acquisitions). During stimulus presentation, anesthetized voles received air flow across the right whiskers; they received no stimuli during baseline and washout (Fig. 8).

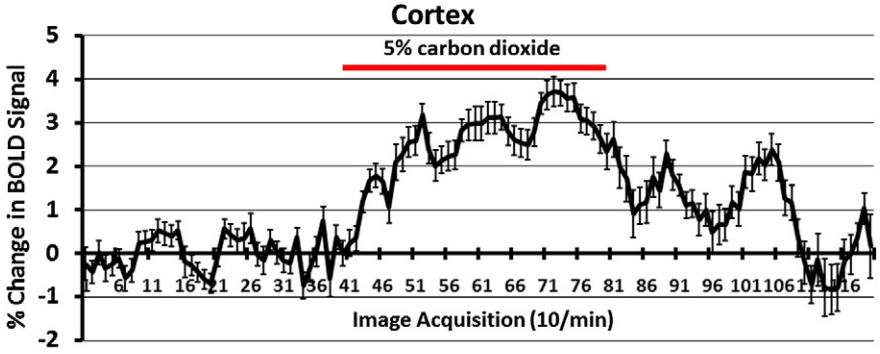

Fig. 7. Shown is a time-course plot (n = 6) for the change in BOLD signal in the cortical mantel in response to a 4 min exposure to 5% CO_2 (red line). Shown are the mean and standard error for each time point.

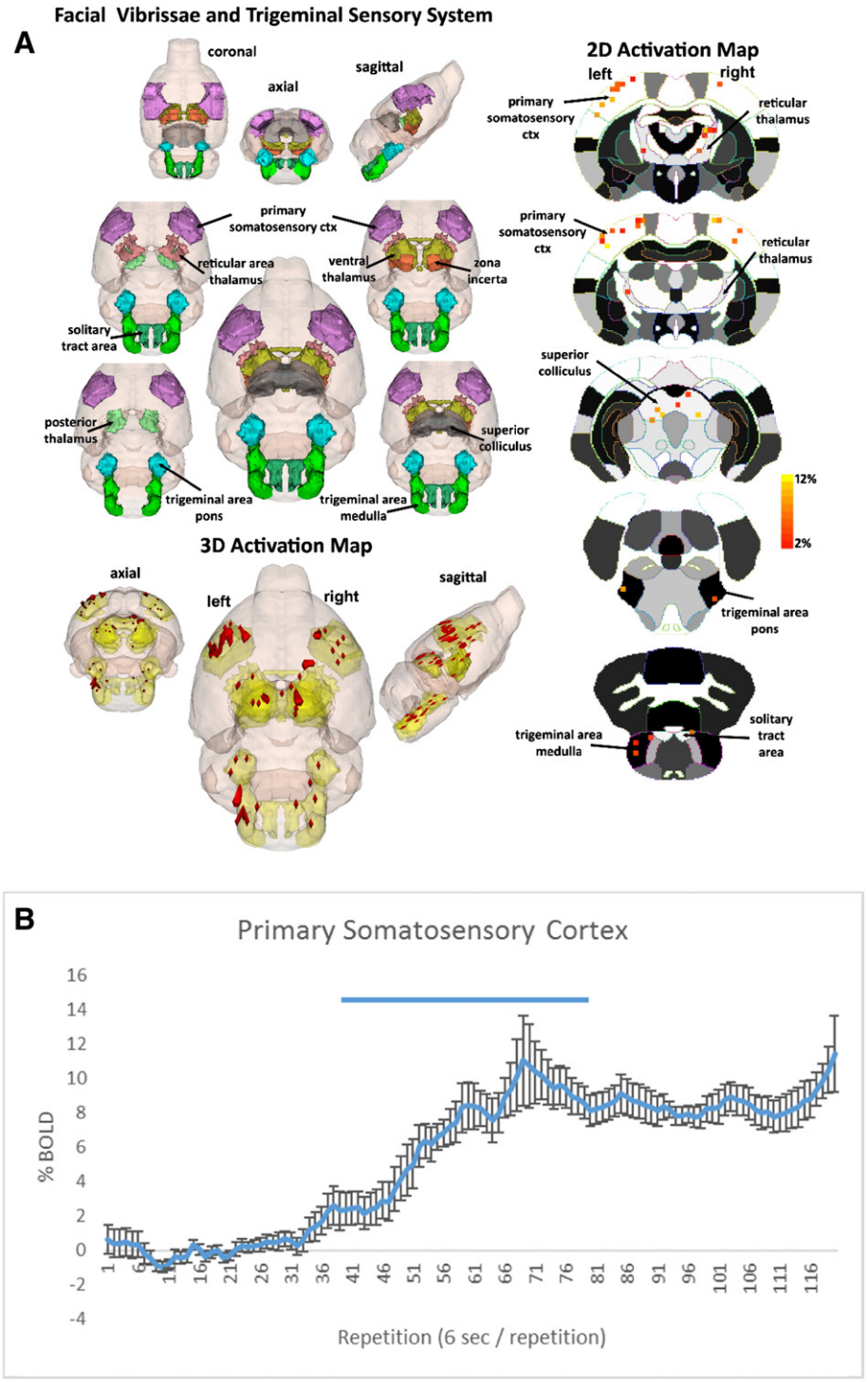

Fig. 8. (A) The 3D color model at the top depicts the location of nine brain areas in the vole comprising the facial vibrissae and trigeminal system. These areas have been coalesced into a single volume (yellow) as shown in the lower 3D images. Areas in red are the localization of the activated voxels comprising the composite average from eight voles exposed to whisker stimulation. Once fully registered and segmented, the statistical responses for each animal are averaged on a voxel-by-voxel bases. Those averaged voxels that are significantly different from baseline for positive BOLD are show in their appropriate spatial location. On the right are 2D activation maps from the vole brain atlas showing the precise location of the significantly altered positive voxels following whisker stimulation. The vertical color strips indicated the percent change in BOLD signal. (B) Timecourse of primary somatosensory cortex BOLD activation. The blue bar represents the duration of whisker stimulation. Error bars represent standard error of the mean.

Novel odor stimulus

Lastly, non-noxious and novel odorants (methyl benzoate, benzaldehyde, and isoamyl acetate) were presented to a separate cohort of awake, non-acclimated adult male voles (n = 8) in order to assess the sensitivity of our methods to innocuous stimuli during awake imaging. Subjects were manually restrained without anesthesia as described above and scanned fully conscious. In the custom-designed head restraint, a bar that holds the incisors in place functions simultaneously as an odor delivery tube. The odor delivery tube is connected by polyethylene tubing to an aquarium pump located outside the magnet

room. As above, scans consisted of three epochs: a 4 min "baseline" epoch, a 4 min "stimulus presentation" epoch, and a 4 min "washout" epoch, for a total of 12 min (120 whole-brain acquisitions). During baseline and washout, all subjects were presented with ambient air at a flow rate of approximately 1.5 lpm. At the start of stimulus presentation, sealed plastic cups containing the odors were placed one at a time into the flow stream. A control group consisted of awake, non-acclimated adult male voles (n = 6) scanned in response to ambient air throughout the entire 12 min scan; brief interruptions in air flow (<2 s) were produced to mimic air flow changes resulting from the transition between epochs. Odorants consisted of methyl benzoate (rosy odor), benzaldehyde (almond odor), and isoamyl acetate (banana odor) (all purchased from Sigma Chemical) prepared as 1% solutions in distilled water. Odors were selected based on our lab's previous experience using them as olfactory stimuli in rats (Kulkarni et al., 2012).

Data analysis

Heart rate, RSA and restraint-induced sounds were compared via repeated measures ANOVA using SPSS v 20.0 (IBM Inc.). When such data were found to violate the assumption of sphericity, a Greenhouse–Geisser correction was applied.

Results

Acclimation

Motion data

The average motion across three dimensions before and after acclimation is presented in Fig. 5. One subject broke its front incisors during acclimation, and as these teeth are critical to proper restraint, this subject was excluded; another subject was injured during restraint and subsequently excluded. Hence, 7 of 9 subjects were available to examine the effects of acclimation on motion. Using the criterion of a single voxel (260 μm) worth of movement for more than a single acquisition, 9 of 9 (100%) of non-acclimated subjects' data were found to be usable, and 0 of 7 (0%) of acclimated subjects' data were found to be usable.

Heart rate/RSA

The cardiovascular effects of restraint are shown in Fig. 6. All 8 subjects were successfully restrained across the five days. During acute (15 min) bouts of restraint, heart rate increased significantly from 395 ± 25 beats per minute (bpm) at baseline to an average of 530 ± 17 bpm during restraint (Fig. 6a; $p < 0.001$) and RSA decreased from an average of 3.26 ± 0.44 $\ln(ms^2)$ to 1.68 ± 0.5 $\ln(ms^2)$ (Fig. 6a; $p < 0.001$). Across the 15 min of restraint, there was a significant effect of time on both heart rates (Fig. 6a; $F_{1.2,17.0} = 24.266$, $p < 0.001$) and RSA (Fig. 6a; $F_{1.2,17.7} = 6.125$, $p = 0.018$), which gradually increased and decreased, respectively. Over the course of the five days of restraint, there were no significant changes in restraint-induced cardioacceleration during the 15 min of restraint in terms of either heart rate or RSA (Fig. 6b, 6c; $p > 0.05$). Likewise, there were no return to baseline differences between days 1 and 5 in terms of either HR or RSA ($p > 0.05$).

The cardioacceleratory response to restraint was similar in magnitude to other common experimental paradigms, namely pup exposure and placement in a wire mesh floored metabolic cage. When adult prairie voles freely interact with an unrelated pup 1–3 days old, heart rate increases to 518 ± 18 bpm. Similarly, upon being placed into a metabolic cage with wire mesh flooring, heart rate increases to 536 ± 47 bpm. There were no significant differences between these three conditions (Fig. 6e; $p > 0.05$).

Vocalizations and restraint-induced sound

Data on restraint-induced sounds are shown in Fig. 6c. All subjects were successfully restrained across the five days. Across 15 min of restraint, voles produced on average 454.4 ± 80.2 sounds, for a total duration of 20.8 ± 4.7 s. The average frequency of the sounds was 12.25 kHz, within the frequency range of human audition. There were no significant differences between the sexes nor between days 1 and 5 in terms of either the number or the total duration of restraint-induced sounds ($p > 0.05$ for all comparisons). Vocalizations almost exclusively occurred within the audible range and coincided with escape attempts. It was unclear whether these vocalizations reflect distress calls or byproducts of struggle with the restraint equipment.

Validation stimuli

Hypercapnic challenge

All subjects (n = 6) were scanned successfully in response to hypercapnic challenge. BOLD signal was broadly increased throughout the brain in response to 5% CO_2 challenge in awake prairie voles. Across all 115 brain regions, BOLD signal was significantly elevated in 13.12 ± 0.9% of voxels, by an average of 5.75 ± 0.24%. Negative BOLD signal, on the other hand, was observed in 2.38 ± 0.54% of voxels, by an average of 1.38 ± 0.17%. The time course for BOLD signal change in activated voxels is shown as a composite of the regions making up the cortical mantle in Fig. 7.

Whisker stimulation

All subjects (n = 8) were successfully scanned for both Whisker and Control conditions. Whisker stimulation while under anesthesia increased BOLD signal in brain regions associated with tactile sensory input, as shown in Fig. 8. The multi-color 3D representation (Fig. 8, *top left*) highlights the relative location of regions that comprise the facial vibrissae and trigeminal sensory systems. With these systems highlighted in yellow, the 3D activation map (Fig. 8, *bottom left*) illustrates significant volumes of activation in red. For closer inspection, 2D activation maps are presented (Fig. 8, *right*), and illustrate significant volumes of activation. Significant activation was noted in the primary somatosensory cortex (predominantly on the left side) and a timecourse of activation in the primary somatosensory cortex is provided to illustrate the temporal structure of BOLD activation.

Novel odor stimulus

One animal from the odor stimulus group was excluded for excessive motion during the scan; all others were scanned successfully. Presentation of the sequence of novel odors (rose/almond/banana) across 4 min elicited BOLD signal increases in various brain regions that comprise the main olfactory system, as shown in Fig. 9. Of the 8 areas demonstrated to be significantly more reactive to novel odors, 4 areas are part of the main olfactory system. These areas include the anterior olfactory area, granular and glomerular layers of the olfactory bulb, and entorhinal cortex. A table listing all activated regions is presented in Fig. 9b.

Discussion

The methods detailed here for fMRI in awake prairie voles present a promising new direction for social, cognitive, and affective neuroscience research. Imaging brain function across time in an awake animal requires that the animal's head is rendered completely stationary. We have developed a set of tools and procedures for achieving this without the potential confounds of prior surgery or anesthesia exposure. Furthermore, the remainder of the animal's body can be left free to move without introducing significant motion artifact. Prairie voles tolerate these imaging conditions, and can be secured for imaging in a manner that is no more invasive or physiologically disruptive than other common procedures employed in normal animal husbandry. Once restrained, voles can have their brains imaged in response to a variety of stimulus provocation paradigms. In the work presented here, we presented voles with a physiological stimulus, inhaled 5% CO_2, and observed indiscriminate positive BOLD change across the entire brain, as

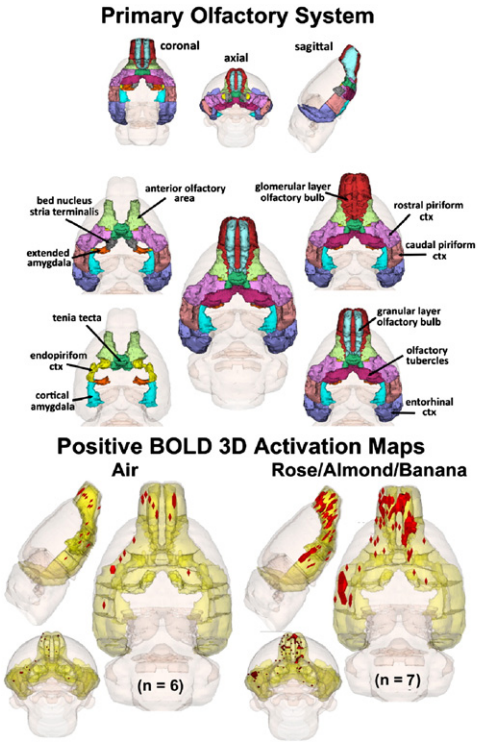

	Air			Rose/Almond/Banana			
B. Region of Interest(ROI)	**median**	**max**	**min**	**median**	**max**	**min**	**P value**
anterior olfactory area	0	4	0	2	29	1	0.015
orbital cortex	0	2	0	2	17	0	0.028
perirhinal cortex	0	2	0	10	12	0	0.029
granular cell layer olfactory bulb	0.5	18	0	6	46	4	0.03
CA1	0	1	0	1	13	0	0.034
auditory cortex	0	2	0	7	19	0	0.036
glomerular layer olfactory bulb	3.5	7	0	8	41	3	0.044
entorhinal cortex	1	7	0	3	36	2	0.051

Fig. 9. (A) The 3D color model at the top depicts the location of the brains that comprise the primary olfactory system in the vole. These areas have been coalesced into a single volume (yellow) as shown in the lower 3D images for ambient air (n = 6) and a sequence of novel odors comprised of rose (methyl benzoate), almond (benzaldehyde), and banana (isoamyl acetate) (n = 7). All odors (Sigma Chemical) were prepared as 1% solutions in distilled water. Localization of the significantly changed positive BOLD voxels comprising the composite average from the voles in each experimental group are shown in red. (B) The table at the bottom lists brain regions rank ordered by statistical significance between subjects presented with ambient air and those presented with the sequence of novel odors.

expected. This observation serves as confirmation that our imaging protocol (including equipment, pulse sequence, and data processing strategy) is capable of detecting an appropriately widespread response to a global change in hypercapnia-induced cerebrovascular dilation. Next, we exposed anesthetized voles to a physical stimulus, unilateral whisker stimulation with an airstream. We observed specific activation of the contralateral somatosensory cortex, confirming that our imaging protocol is capable of isolating precise changes in neural function.

Finally, we sought to determine whether our awake imaging methodology would have the capacity to uncover changes in neural activation resulting from the perception of novel odorants. After exposing voles to a sequence of non-noxious, novel odors, including methyl benzoate (rose), benzaldehyde (almond), and isoamyl acetate (banana) we observed increased activation in brain regions that comprise the main olfactory system, including the anterior olfactory area, granular and glomerular cell layers of the olfactory bulb, and the entorhinal cortex (at the level of statistical trend). The increased BOLD activation also seen in the perirhinal cortex and auditory cortex suggest that the presentation of novel odors within our awake imaging paradigm also recruited areas involved in the integration of information from multiple sensory inputs. The increased BOLD activation seen in the orbital cortex and CA1 of the hippocampus were unexpected and the involvement of these areas in the perception of novel odors is intriguing and begs further study. Taken together, these data confirmed that our awake imaging procedures, even in the absence of stress habituation, were successful in visualizing BOLD activation in the main olfactory system in response to the perception of novel odors.

Neuroimaging in awake rodents has traditionally required acclimation to restraint procedures for two reasons: to ensure stability during image acquisition and to minimize distress. Based on the observed effects of repeated restraint in conditions similar to imaging, we conclude that prairie voles do not acclimate to such conditions. Motion during scanning was within acceptable bounds for the vast majority of subjects on their first day of imaging, whereas subjects that had been restrained 5 days in a row in a mock scanner actually showed greater motion during scans, and hence produced unusable data. Furthermore, none of physiological or behavioral measures of arousal indicated any decrements over the course of the 5 days (heart rate, RSA, or s/restraint-induced sounds). Based on the minimal motion artifact generated on the first day of restraint and the observed responses to repeated restraint, we recommend that imaging can take place with animals naïve to imaging conditions, and that repeated scans of the same animal

can lead to difficulties in maintaining image stability, even across relatively short scans. Conducting fewer scans on the same animal and/or providing extra recovery time in the interval may allow for repeated scans.

The lack of changes in baseline HR and RSA is important in that it suggests repeated restraint is not producing enduring changes in the animals' autonomic state. The lack of acclimation during restraint is at odds with previously observed findings in rats (King et al., 2005; Upadhyay et al., 2011), which exhibit habituation to repeated restraint. There are several possible explanations for this discrepancy. For example, the restraint hardware is necessarily different to accommodate differences in size between the species. Another potential factor is that of differences between the species themselves. Rats and voles may differ along any number of dimensions related to temperament, arousal/reactivity, or even learning/memory. Prairie voles are not far removed from wild caught animals, while laboratory rats have been selectively bred over hundreds of generations for docility, and hence respond differently to many typical research interventions. It is likely that voles experience a high level of arousal during many commonly used testing paradigms. For example, the maximal heart rate observed during restraint is no different than that displayed during unfettered interaction with a 1–3 day old pup (Kenkel et al., 2015) or while spending time in a novel metabolic cage with wire mesh floor.

No careful observation should disregard the initial state of its subject. Therefore, any discussion of neuroimaging findings in awake prairie voles should be preceded by a careful consideration of the environmental context during imaging. In our best attempts to acclimate voles to the imaging environment, we were unable to demonstrate habituation to the experience of head restraint required for satisfactory images. While it would no doubt be ideal to provide voles with a completely "stress-free" imaging environment, as many of our colleagues have expressed (Febo, 2015), we have come to the preliminary conclusion that our initial expectation to remove stress from the imaging context was unrealistic, particularly for an animal model only a few generations from being wild-caught. In none of the parameters measured were we able to find any evidence for voles acclimating to the conditions of head restraint. Some signs point towards a relatively low level of stress as compared with other common laboratory procedures (see Fig. 6d, tachycardic response to head restraint is equivalent to placement in mesh-floor metabolic cages), however, we feel it would be on the whole disingenuous to argue that our current method of nearly complete head restraint in a nearly wild rodent is free from psychological stress. Rather, we recommend proceeding with a clear understanding that the initial state of our subjects includes an element of psychological stress. Therefore, future applications of fMRI in prairie voles will take advantage of this property to further our understanding of stress regulation in socially monogamous and biparental species.

In summary, we have developed a set of procedures, including custom head-restraint equipment, quadrature RF coil, pulse sequence, 3D segmented atlas, and data processing strategy, which allows functional neuroimaging without prior surgery or the use of anesthesia. Using these procedures we have demonstrated the ability to visualize the neural response to a cascade of novel odors in awake prairie voles. While we were unable to demonstrate habituation to repeated restraint as seen in other rodents, we were able to show on the initial imaging-restraint session that prairie voles will hold still enough to permit visualization of the response to novel odors. Taken together, these studies demonstrate the potential of fMRI in awake animals as a new platform for the integrative study of animal behavior (Rubenstein et al., 2014).

Conflict of interest

Craig Ferris has a financial interest in Animal Imaging Research, the company that developed the vole imaging system. Craig Ferris and Praveen Kulkarni have a financial interest in Ekam Solutions the company that developed the vole MRI atlas. The other authors declare no conflicts of interest.

Acknowledgements

These studies were supported by a grant from the National Institute of Childhood Health and Human Development NICHD P01HD075750.

References

Sixth report on the statistics on the number of animals used for experimental and other scientific purposes in the Member States of the European Union, 2010e. Report from the Commission to the Council and the European Parliament. COM (511 final, 30 September 2010 [WWW Document], 2010. URL http://aei.pitt.edu/33392/ accessed 12.3.15).

Bohrer, R.E., Porges, S.W., 1982. The application of time-series statistics to psychological research: an introduction. Psychol. Stat. Lawrence Erlbaum Assoc. Hillsdale NJ 309–345.

Brevard, M.E., Duong, T.Q., King, J.A., Ferris, C.F., 2003. Changes in MRI signal intensity during hypercapnic challenge under conscious and anesthetized conditions. Magn. Reson. Imaging 21, 995–1001.

Davis, M., Whalen, P.J., 2001. The amygdala: vigilance and emotion. Mol. Psychiatry 6, 13–34. http://dx.doi.org/10.1038/sj.mp.4000812.

Dingemanse, N.J., Kazem, A.J.N., Réale, D., Wright, J., 2010. Behavioural reaction norms: animal personality meets individual plasticity. Trends Ecol. Evol. 25, 81–89. http://dx.doi.org/10.1016/j.tree.2009.07.013.

Duong, T.Q., Yacoub, E., Adriany, G., Hu, X., Uğurbil, K., Kim, S.-G., 2003. Microvascular BOLD contribution at 4 and 7 T in the human brain: gradient-echo and spin-echo fMRI with suppression of blood effects. Magn. Reson. Med. 49, 1019–1027.

Everitt, B.J., 1990. Sexual motivation: a neural and behavioural analysis of the mechanisms underlying appetitive and copulatory responses of male rats. Neurosci. Biobehav. Rev. 14, 217–232. http://dx.doi.org/10.1016/S0149-7634(05)80222-2.

Febo, M., 2015. A new day for an old emotion: studying fear learning using awake mouse functional magnetic resonance imaging (commentary on Harris et al.). Eur. J. Neurosci. 42, 2123–2124. http://dx.doi.org/10.1111/ejn.13014.

Febo, M., Ferris, C.F., 2007. Development of cocaine sensitization before pregnancy affects subsequent maternal retrieval of pups and prefrontal cortical activity during nursing. Neuroscience 148, 400–412. http://dx.doi.org/10.1016/j.neuroscience.2007.05.026.

Febo, M., Segarra, A.C., Tenney, J.R., Brevard, M.E., Duong, T.Q., Ferris, C.F., 2004. Imaging cocaine-induced changes in the mesocorticolimbic dopaminergic system of conscious rats. J. Neurosci. Methods 139, 167–176. http://dx.doi.org/10.1016/j.jneumeth.2004.04.028.

Febo, M., Ferris, C.F., Segarra, A.C., 2005. Estrogen influences cocaine-induced blood oxygen level-dependent signal changes in female rats. J. Neurosci. 25, 1132–1136. http://dx.doi.org/10.1523/JNEUROSCI.3801-04.2005.

Ferris, C.F., Kulkarni, P., Sullivan, J.M., Harder, J.A., Messenger, T.L., Febo, M., 2005. Pup suckling is more rewarding than cocaine: evidence from functional magnetic resonance imaging and three-dimensional computational analysis. J. Neurosci. 25, 149–156. http://dx.doi.org/10.1523/JNEUROSCI.3156-04.2005.

Ferris, C.F., Stolberg, T., Kulkarni, P., Murugavel, M., Blanchard, R., Blanchard, D.C., Febo, M., Brevard, M., Simon, N.G., 2008. Imaging the neural circuitry and chemical control of aggressive motivation. BMC Neurosci. 9, 111. http://dx.doi.org/10.1186/1471-2202-9-111.

Ferris, C.F., Smerkers, B., Kulkarni, P., Caffrey, M., Afacan, O., Toddes, S., Stolberg, T., Febo, M., 2011. Functional magnetic resonance imaging in awake animals. Rev. Neurosci. 22, 665–674. http://dx.doi.org/10.1515/RNS.2011.050.

Ferris, C.F., Kulkarni, P., Toddes, S., Yee, J., Kenkel, W., Nedelman, M., 2014. Studies on the Q175 knock-in model of Huntington's disease using functional imaging in awake mice: evidence of olfactory dysfunction. Front. Neurol. 5, 94. http://dx.doi.org/10.3389/fneur.2014.00094.

Fuller, T., Sarkar, S., Crews, D., 2005. The use of norms of reaction to analyze genotypic and environmental influences on behavior in mice and rats. Neurosci. Biobehav. Rev. 29, 445–456. http://dx.doi.org/10.1016/j.neubiorev.2004.12.005.

Genovese, C.R., Lazar, N.A., Nichols, T., 2002. Thresholding of statistical maps in functional neuroimaging using the false discovery rate. NeuroImage 15, 870–878.

Grippo, A.J., Lamb, D.G., Carter, C.S., Porges, S.W., 2007. Cardiac regulation in the socially monogamous prairie vole. Physiol. Behav. 90, 386–393. http://dx.doi.org/10.1016/j.physbeh.2006.09.037.

Kenkel, W.M., Paredes, J., Lewis, G.F., Yee, J.R., Pournajafi-Nazarloo, H., Grippo, A.J., Porges, S.W., Carter, C.S., 2013. Autonomic substrates of the response to pups in male prairie voles. PLoS One 8, e69965. http://dx.doi.org/10.1371/journal.pone.0069965.

Kenkel, W.M., Yee, J.R., Porges, S.W., Ferris, C.F., Carter, C.S., 2015. Cardioacceleration in alloparents in response to stimuli from prairie vole pups: the significance of thermoregulation. Behav. Brain Res. 286, 71–79. http://dx.doi.org/10.1016/j.bbr.2015.02.033.

Kenkel, W.M., Yee, J.R., Moore, K., Madularu, D., Kulkarni, P., Gamber, K., Nedelman, M., Ferris, C.F., 2016. Functional magnetic resonance imaging in awake transgenic fragile X rats: evidence of dysregulation in reward processing in the mesolimbic/habenular neural circuit. Transl. Psychiatry 6, e763. http://dx.doi.org/10.1038/tp.2016.15.

King, J.A., Garelick, T.S., Brevard, M.E., Chen, W., Messenger, T.L., Duong, T.Q., Ferris, C.F., 2005. Procedure for minimizing stress for fMRI studies in conscious rats. J. Neurosci. Methods 148, 154–160. http://dx.doi.org/10.1016/j.jneumeth.2005.04.011.

Kramer, K.M., Cushing, B.S., Carter, C.S., Wu, J., Ottinger, M.A., 2004. Sex and species differences in plasma oxytocin using an enzyme immunoassay. Can. J. Zool.-Rev. Can. Zool. 82, 1194–1200. http://dx.doi.org/10.1139/Z04-098.

Kulkarni, P.P., Sullivan, J.M., Ghadyani, H.R., Huang, W., Wu, Z., King, A., 2003. Automatic Segmentation of a Rat Brain Atlas via a Multiple-material Marching Cube Strategy, in: Proc. Intl. Soc. Mag. Reson, Med.

Kulkarni, P., Stolberg, T., Sullivanjr, J.M., Ferris, C.F., 2012. Imaging evolutionarily conserved neural networks: preferential activation of the olfactory system by food-related odor. Behav. Brain Res. 230, 201–207. http://dx.doi.org/10.1016/j.bbr.2012.02.002.

Lahti, K.M., Ferris, C.F., Li, F., Sotak, C.H., King, J.A., 1998. Imaging brain activity in conscious animals using functional MRI. J. Neurosci. Methods 82, 75–83.

Lewis, G.F., Furman, S.A., McCool, M.F., Porges, S.W., 2012. Statistical strategies to quantify respiratory sinus arrhythmia: are commonly used metrics equivalent? Biol. Psychol. 89, 349–364. http://dx.doi.org/10.1016/j.biopsycho.2011.11.009.

Lorenz, K.Z., 1950. The Comparative Method in Studying Innate Behavior Patterns.

Madularu, D., Yee, J.R., Kenkel, W.M., Moore, K.A., Kulkarni, P., Shams, W.M., Ferris, C.F., Brake, W.G., 2015. Integration of neural networks activated by amphetamine in females with different estrogen levels: a functional imaging study in awake rats. Psychoneuroendocrinology 56, 200–212. http://dx.doi.org/10.1016/j.psyneuen.2015.02.022.

Norris, D.G., 2012. Spin-echo fMRI: the poor relation? NeuroImage 62, 1109–1115.

Paxinos, G., Franklin, K.B., 2004. The Mouse Brain in Stereotaxic Coordinates. Gulf Professional Publishing.

Phillips, R., Ledoux, J., 1992. Differential contribution of amygdala and hippocampus to cued and contextual fear conditioning. Behav. Neurosci. 106, 274–285. http://dx.doi.org/10.1037//0735-7044.106.2.274.

Porges, S.W., 1985. Method and Apparatus for Evaluating Rhythmic Oscillations in Aperiodic Physiological Response Systems. US4510944 A.

Rubenstein, D.R., Hofmann, H., Akcay, E., Alonzo, A., Archie, E., Beery, A., Calisi-Rodríguez, R., Carleton, K., Chow, B., Dubnau, J., 2014. New frontiers for the integrative study of animal behavior. White Pap. Rep. Natl. Sci. Found.http://www.nsf.gov/bio/pubs/reports/New_Frontiers_for_the_Integrative_Study_of_Animal_Behavior_workshop_report.pdf

Schmalhausen, I.I., 1949. Factors of Evolution: the Theory of Stabilizing Selection.

Schneirla, T.C., 1949. Levels in the Psychological Capacities of Animals.

Sicard, K., Shen, Q., Brevard, M.E., Sullivan, R., Ferris, C.F., King, J.A., Duong, T.Q., 2003. Regional cerebral blood flow and BOLD responses in conscious and anesthetized rats under basal and hypercapnic conditions: implications for functional MRI studies. J. Cereb. Blood Flow Metab. Off. J. Int. Soc. Cereb. Blood Flow Metab. 23, 472–481.

Smiseth, P.T., Wright, J., Kölliker, M., 2008. Parent–offspring conflict and co-adaptation: behavioural ecology meets quantitative genetics. Proc. R. Soc. Lond. B Biol. Sci. 275, 1823–1830. http://dx.doi.org/10.1098/rspb.2008.0199.

Stoesz, B.M., Hare, J.F., Snow, W.M., 2013. Neurophysiological mechanisms underlying affiliative social behavior: insights from comparative research. Neurosci. Biobehav. Rev. 37, 123–132. http://dx.doi.org/10.1016/j.neubiorev.2012.11.007.

Strickland, J.C., Smith, M.A., 2015. Animal models of social contact and drug self-administration. Pharmacol. Biochem. Behav. 136, 47–54. http://dx.doi.org/10.1016/j.pbb.2015.06.013.

Swanson, L.W., 2004. Brain maps: structure of the rat brain (2nd edn). Nature 363, 347–350.

Tenney, J.R., Duong, T.Q., King, J.A., Ferris, C.F., 2004. FMRI of brain activation in a genetic rat model of absence seizures. Epilepsia 45, 576–582. http://dx.doi.org/10.1111/j.0013-9580.2004.39303.x.

Tinbergen, N., 1963. On aims and methods of ethology. Z. Für Tierpsychol. 20, 410–433.

Ugurbil, K., Adriany, G., Andersen, P., Chen, W., Gruetter, R., Hu, X.P., Merkle, H., Kim, D.S., Kim, S.G., Strupp, J., Zhu, X.H., Ogawa, S., 2000. Magnetic resonance studies of brain function and neurochemistry. Annu. Rev. Biomed. Eng. 2, 633–660. http://dx.doi.org/10.1146/annurev.bioeng.2.1.633.

Upadhyay, J., Baker, S.J., Chandran, P., Miller, L., Lee, Y., Marek, G.J., Sakoglu, U., Chin, C.-L., Luo, F., Fox, G.B., Day, M., 2011. Default-mode-like network activation in awake rodents. PLoS One 6, e27839. http://dx.doi.org/10.1371/journal.pone.0027839.

Yacoub, E., Duong, T.Q., De Moortele, V., Lindquist, M., Adriany, G., Kim, S.-G., Uğurbil, K., Hu, X., et al., 2003. Spin-echo fMRI in humans using high spatial resolutions and high magnetic fields. Magn. Reson. Med. 49, 655–664.

Yacoub, E., Shmuel, A., Logothetis, N., Uğurbil, K., 2007. Robust detection of ocular dominance columns in humans using Hahn spin echo BOLD functional MRI at 7 Tesla. NeuroImage 37, 1161–1177. http://dx.doi.org/10.1016/j.neuroimage.2007.05.020.

Yee, J.R., Kenkel, W., Caccaviello, J.C., Gamber, K., Simmons, P., Nedelman, M., Kulkarni, P., Ferris, C.F., 2015. Identifying the integrated neural networks involved in capsaicin-induced pain using fMRI in awake TRPV1 knockout and wild-type rats. Front. Syst. Neurosci. 9, 15. http://dx.doi.org/10.3389/fnsys.2015.00015.